

Univerza v Ljubljani
Fakulteta za *matematiko in fiziko*



ATLAS jet measurements with different R

Jure Aplinc, dipl. fiz. (UN)

SUPERVISOR:
dr. Pavel Starovoitov

6th September 2012

Abstract

At the Large Hadron Collider (LHC), jet production is the dominant high transverse momentum (p_t) process. Jet cross sections serve as the main observables in high-energy particle physics, providing precise information on the structure of the proton. They are important tool for understanding the strong interaction and searching for possible physics beyond the Standard Model. In this paper definition and properties of a jet will be presented. We will introduce the jet clustering algorithm and compare results for two different values of jet radius, which is free parameter of the algorithm.

Contents

1	Introduction	2
2	Jet clustering algorithm	2
3	Analysis of the ATLAS jet measurements with different R	4
3.1	Δp_t distribution	5
3.2	Correlation between $p_t(R = 0.4)$ and $p_t(R = 0.6)$	6
4	Conclusion	7

1 Introduction

Protons are collided at LHC in order to produce new particles and therefore check existing theories and possibly to discover new, so far unknown, phenomena. Currently accepted theory of strong interaction between particles that carry color is Quantum Chromodynamics (QCD).

When protons collide only one of the partons in the first proton interact with one of the partons in the other proton. These particles are called quarks and gluons, they carry only a fraction of the proton momentum. After collision new partons are created, but due to confinement of strong interaction, they hadronize into mesons and barions (color singlets). Most of those products are unstable and eventually decay into more stable ones. Obviously we can't detect directly partons (quarks q and gluons g) in the detector, but we can detect particles after hadronization (π , K, e, μ , γ , ...) or jets (sprays) [1] [2].

If we are interested in gluons and quarks we are not interested in to all hadronization and decay products. So we combine all those relatively collinear particles into one jet. A jet is therefore represented by a fourvector, the sum of all fourvectors of the jet constituents.

2 Jet clustering algorithm

Usually we are dealing with more than just one jet and they can partially overlap, so it is not trivial to cluster particles, belonging to the same jet together (fig. 1).

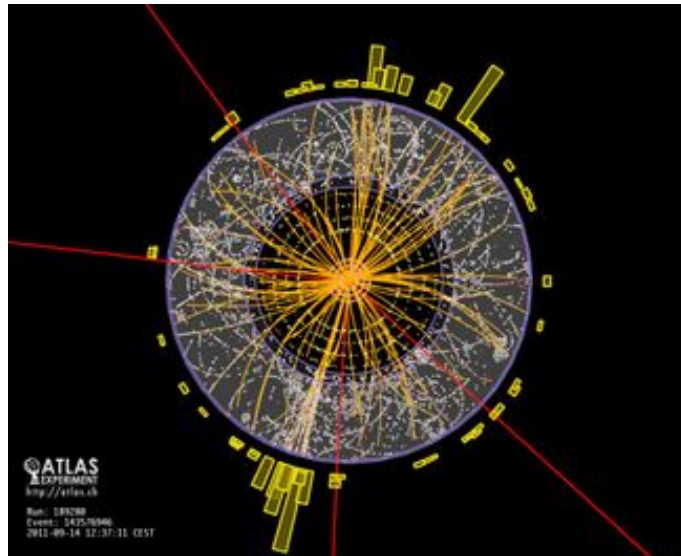


Figure 1: Picture of proton-proton collision from LHC measured by ATLAS detector. We can see high number of the particle tracks, but one can't easily decide how to cluster them in to jets.

Therefore jet clustering algorithms have been developed, to do this work automatically. There are several clustering algorithms for example [3]:

- SISCone jet clustering algorithm
- k_t jet clustering algorithm
- Cambridge-Aachen jet clustering algorithm
- anti- k_t jet clustering algorithm.

Last three algorithms are strongly related to one another and will be briefly explained below.

As usual, one introduces distances d_{ij} between entities (particles, pseudojets) i and j and d_{iB} between entity i and the beam (B) [3]. The (inclusive) clustering proceeds by identifying the smallest of the distances and if it is a d_{ij} recombining entities i and j , while if it is d_{iB} calling i a jet and removing it from the list of entities. The distances are recalculated and the procedure repeated until no entities are left. The extension relative to the k_t , anti- k_t and Cambridge/Aachen algorithms lies in our definition of the distance measures:

$$d_{ij} = \min \left(k_{ti}^{2p}, k_{tj}^{2p} \right) \frac{\Delta_{ij}^2}{R^2}, \quad (2.0.1)$$

$$d_{iB} = k_{ti}^{2p}, \quad (2.0.2)$$

where

$$\Delta_{ij}^2 = (y_i - y_j)^2 + (\phi_i - \phi_j)^2 \quad (2.0.3)$$

and k_{ti} , y_i and ϕ_i are respectively the transverse momentum, rapidity and azimuth of particle i . In addition to the usual radius R , we have added a parameter p to govern the relative power of the energy versus geometrical (Δ_{ij}) scales.

For $p = 1$ one recovers the inclusive k_t algorithm. It can be shown in general that for $p > 0$ the behaviour of the jet algorithm with respect to soft radiation is rather similar to that observed for the k_t algorithm, because what matters is the ordering between particles and for finite Δ this is maintained for all positive values of p . The case of $p = 0$ is special and it corresponds to the inclusive Cambridge/Aachen algorithm. Negative values of p might at first sight seem pathological. We shall see that they are not. The behaviour with respect to soft radiation will be similar for all $p < 0$, so here we will concentrate on $p = -1$, and refer to it as the "anti- k_t " jet-clustering algorithm.

The behaviours of different jet algorithms are illustrated in fig. 1.

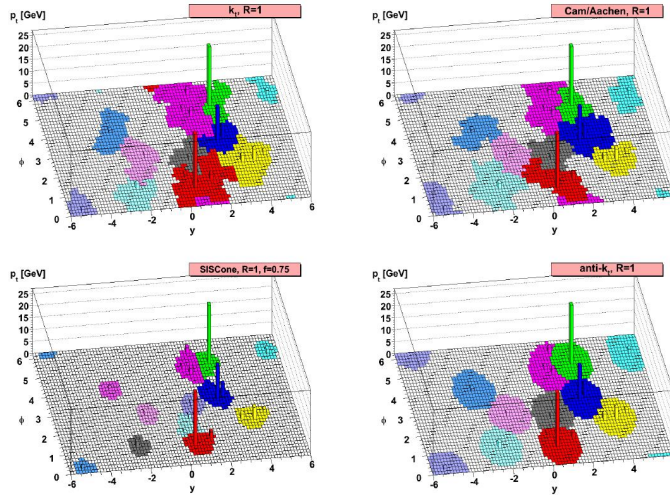


Figure 2: We have some partonic level events together with 10^4 random soft particles. They are clustered with all four mentioned clustering algorithms with the same parameter R . For each of the partonic jets, the region within which random soft particles are clustered in that jet [3].

SIScone (and Cambridge/Aachen) place the boundary between the jets roughly midway between them. Anti- k_t algorithm instead generates a circular hard jet, which covers a lens-shaped region out of the soft one [3].

3 Analysis of the ATLAS jet measurements with different R

The ATLAS collaboration is using anti- k_t algorithm for jets definition. Since radius of the jet is a free parameter one can arbitrary choose its values. The jet clustering in ATLAS experiment is performed for two different radii $R = 0.4$ and $R = 0.6$. Of course, we can expect that we won't find the same number of jets (in one event) using different parameters, furthermore jet found by using radius $R = 0.4$ will differ from corresponding jet with $R = 0.6$ in p_t (because number of particles included in single jet correlate with its size). Distances between jets in both sets for Monte Carlo simulations and data are shown in fig. 3, distances between positions of corresponding jets in both sets are shown and fig. 4.

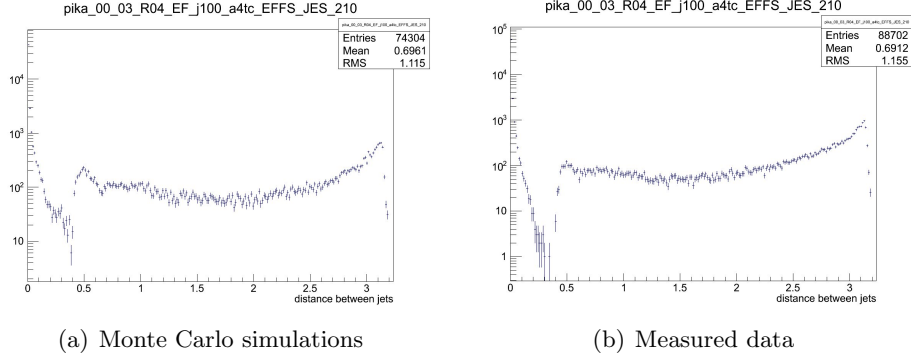


Figure 3: (a) Distances between jets from the same event. Events on the plot are simulated with monte carlo simulations. (b) Minimal distances between two corresponding jets from the same event. Events on the plot are simulated with Monte Carlo simulations.

We can see that there is great similarity among the distributions on fig. 3 of distances between all jets for Monte Carlo simulations (a) and measured data (b).

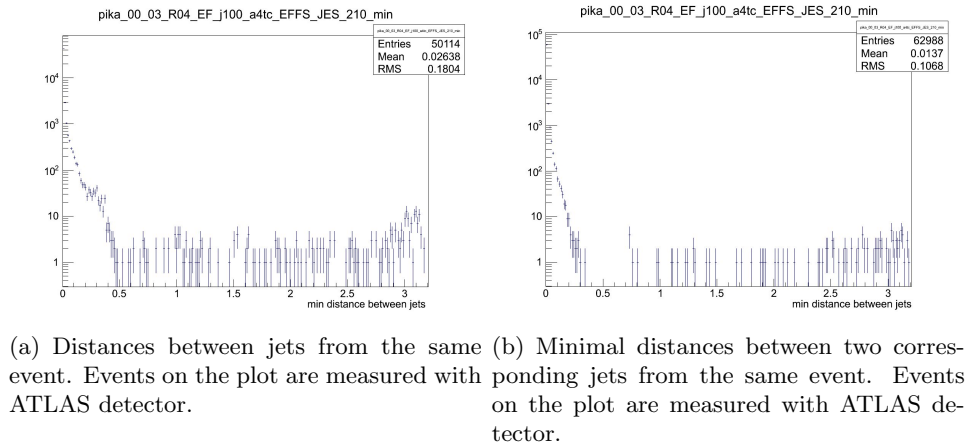


Figure 4: On histograms (a) and (b) we have plots of distances (on unit sphere) between corresponding jets in both sets.

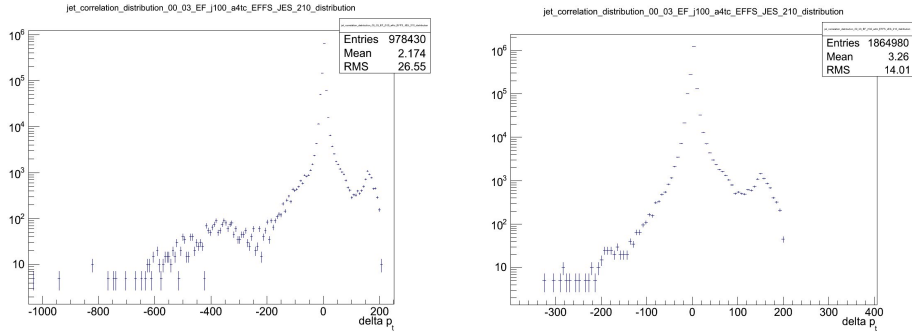
The most events on fig. 4 is centered around 0, that means that the position of the jet from set with $R = 0.4$ match very well with the one for jet with $R = 0.6$. In both cases the small peak

near π can be observed, that is the consequence of back to back electrons. Presented histograms are limited in rapidity $0 < \eta < 0.3$ and in transverse momentum $210 \text{ GeV} < p_t < 260 \text{ GeV}$.

It is interesting to compare the jets properties, produced by anti- k_t algorithm with different radii R .

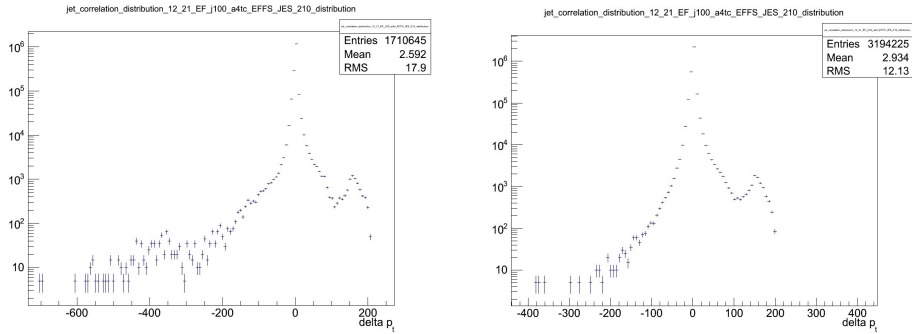
3.1 Δp_t distribution

A simple algorithm has been developed to find corresponding jets in both sets, those jets should differ in the transverse momentum (p_t), as we assumed before. So we check $\Delta p_t = p_t(R = 0.6) - p_t(R = 0.4)$ for each jet in event for many events. Histograms have been produced, showing Δp_t distribution with entries from Monte Carlo simulations (fig. 5 a and fig. 6 a) and experimental data (fig. 5 b and fig. 6 b).



(a) Distribution of Δp_t . Events on the plot are simulated with Monte Carlo simulations. (b) Distribution of Δp_t . Events on the plot are measured with ATLAS detector.

Figure 5: Obviously there is a big similarity between Monte Carlo simulations and measured data. Histograms are limited in rapidity $0 < \eta < 0.3$ and in transverse momentum $210 \text{ GeV} < p_t < 260 \text{ GeV}$.



(a) Distribution of Δp_t . (b) Distribution of Δp_t .

Figure 6: Distribution of δp_t for Events on the plots are simulated with Monte Carlo simulations (a) and measured with ATLAS detector (b).

Obviously there is a big similarity between Monte Carlo simulations and measured data. Histograms are limited in rapidity $0 < \eta < 0.3$ and in transverse momentum $210 \text{ GeV} < p_t < 260 \text{ GeV}$.

One can see that in both cases the center of distribution is centered a little more to the positive side, because $p_t(R = 0.6)$ is in most cases bigger than $p_t(R = 0.4)$.

3.2 Correlation between $p_t(R = 0.4)$ and $p_t(R = 0.6)$

In previous subsection we discovered, that transverse momentum p_t for jets with radius $R = 0.4$ and $R = 0.6$ slightly differs. It is also of a great interest to test the correlation between p_t of jet with radius $R = 0.4$ and $R = 0.6$. We hope that decision for radius of a jet will not affect on the physics results, so strong correlation is expected.

Correlation between jets with radius $R = 0.4$ and $R = 0.6$ is plotted on fig. 7 for $0 < \eta < 0.3$ and 8 for $1.2 < \eta < 2.1$.

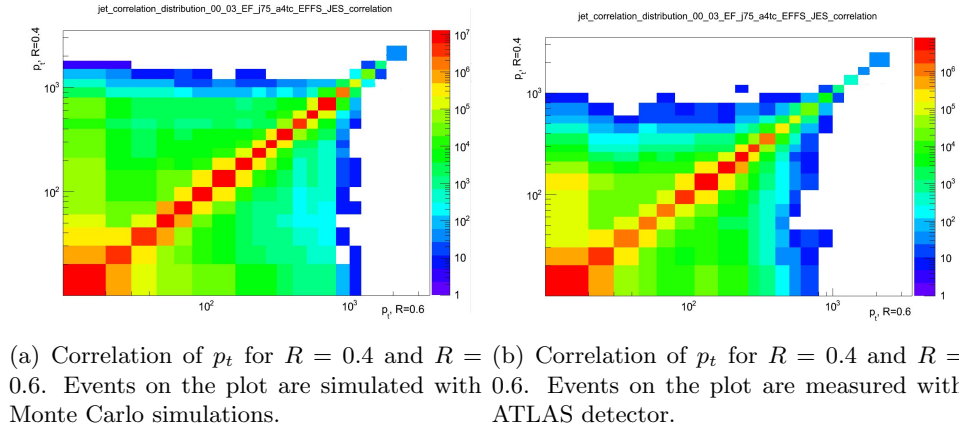


Figure 7: Histograms contains data for $0 < \eta < 0.3$. On fig. a we have correlation for Monte Carlo events, on fig. b for measured data.

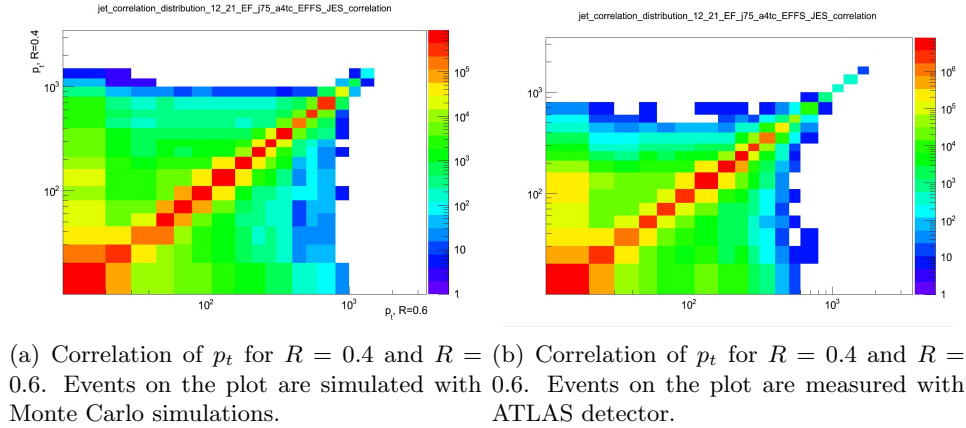


Figure 8: Histograms contains data for $1.2 < \eta < 2.1$. On fig. a we have correlation for Monte Carlo events, on fig. b for measured data.

p_t 's between $R = 0.4$ and $R = 0.6$ are very well correlated (for both rapidity bins), since the most entries lie on 45° angle, as can be seen from enclosed figures. The entries that lie exactly on the line, lie in the peak of the distributions fig. 5 and 6 But of course there are some entries outside the line, those corresponds to the tails in mentioned distributions. In

previous subsection we discovered, that distributions are not centered on zero, but slightly to the positive side due to different p_t 's of jets with different radii. We can see this on correlation histograms as small asymmetry, more events can be found near $R = 0.4$ axis and small transverse momentum for $R = 0.6$ parameter.

It can be deduced from the histograms, that p_t 's are stronger correlated for larger transverse momenta, and less for smaller. Correlation is observed to be stronger in Monte Carlo events, compared to the measured data.

4 Conclusion

With our analysis we investigated the radius dependency of anti- k_t algorithm, which is used by ATLAS corporation for jet clustering. We discovered, that transverse momenta for jets clustered with different radii slightly differs, due to the number of particles contained into the jet.

This is directly connected with p_t correlation between jets. We mainly observe very strong correlation, especially for larger p_t , but also small asymmetry due to different number of particles contained into the jet and therefore different p_t .

References

- [1] A. R. Baden *Jets and kinematics in hadronic collisions*, Int. Jour. Mod. Phys. (1997).
- [2] The ATLAS Collaboration *Measurement of inclusive jet and dijet production in pp collisions at $\sqrt{s} = 7$ TeV using the ATLAS detector*, Phys. Rev. **192**, (2011).
- [3] M Cacciari, G. P. Salam and G. Soyez *The anti- k_t jet clustering algorithm*, LPTHE-07-03, (2008)